Inter*net* Electronic Journal of Molecular Design

March 2003, Volume 2, Number 3, Pages 179–194

Editor: Ovidiu Ivanciuc

Special issue dedicated to Professor Haruo Hosoya on the occasion of the 65th birthday
Part 7

Guest Editor: Jun–ichi Aihara

The Solvent Boundary Potential: A New Approach for Computer Simulation of Large Systems

Valentin Gogonea

Department of Chemistry, Cleveland State University, 2121 Euclid Avenue, Cleveland, Ohio 44115

Received: January 10, 2003; Accepted: February 23, 2003; Published: March 31, 2003

Citation of the article:
V. Gogonea, The Solvent Boundary Potential: A New Approach for Computer Simulation of Large Systems, *Internet Electron. J. Mol. Des.* **2003**, *2*, 179–194, http://www.biochempress.com.

Inter*net* Electronic Journal of Molecular Design

BioChem Press
http://www.biochempress.com

The Solvent Boundary Potential: A New Approach for Computer Simulation of Large Systems[#]

Valentin Gogonea*

Department of Chemistry, Cleveland State University, 2121 Euclid Avenue, Cleveland, Ohio 44115

Received: January 10, 2003; Accepted: February 23, 2003; Published: March 31, 2003

Internet Electron. J. Mol. Des. **2003**, *2* (3), 179–194

Abstract

The paper presents the theoretical framework for the development of a new solvent boundary method for computer simulations and its possible application to the simulation of nitric oxide synthase. Different approaches for the construction of a solvent boundary potential are reviewed and their strengths and weaknesses are discussed. A new solvent boundary potential is proposed which combines the mean field force approximation with the Green's function approach for treating long–range electrostatic interactions, and introduces a novel strategy to treat electrostriction effects due to ions crossing the solvent boundary. Finally, a series of computational tests are devised in order to assess the validity and efficiency of the new solvent boundary potential.

Keywords. Solvent boundary potential; molecular dynamics; mean field force approximation.

Abbreviations and notations

SBP, solvent boundary potential	MFF, mean field force
PBC, periodic boundary conditions	QM/MM, quantum mechanical molecular mechanics
MFFA, mean field force approximation	PMF, potential of the mean force
GSBP, generalized solvent boundary potential	NOS, nitric oxide synthase
DSBC, dynamic surface boundary conditions	SBC, spherical boundary conditions
SCAAS, surface–constrained all–atom solvent	MD, molecular dynamics
RFE, reaction field with exclusion	

1 INTRODUCTION

Today the study of the behavior and properties of condensed phase species by computer simulation methods is common practice [1,2]. However, such an approach still needs many computational resources because it requires the calculation of a detailed trajectory for a large number of solvent molecules. A computer simulation must employ periodic boundary conditions (PBC) in order to properly describe the long–range electrostatic interactions. In the case of simulating heterogeneous systems, such as amorphous solids, clusters, macromolecules in solution, and interfaces, PBC do not adequately describe the interactions because they have the tendency to

[#] Dedicated to Professor Haruo Hosoya on the occasion of the 65th birthday.

* Correspondence author; phone: 216–875–9717; fax: 216–687–9298; E–mail: v.gogonea@csuohio.edu.

impose a long–range order [2]. In addition, the solute can be very large and will require many thousands of solvent molecules to 'wrap' it into a simulation box. Because these difficulties were recognized in the early stages of the development of computer simulation methods, a solvent boundary potential (SBP) was proposed as an alternative to PBC [3–10]. While the SBP has not yet found its way into the mainstream of computer simulation algorithms which are currently implemented in popular computer simulation programs based on force fields such as AMBER [11], CHARMM [12], or GROMOS [13] there is definitely a revived interest in this new approach [8–10].

Examples of early developments of a SBP approach can be found in the works of Stace and Murrel [3], Northrup [14], Tenenbaum *et*. *al*. [15], Berkowitz and McCammon [4], and Brooks III and Karplus [5]. For example, Stace and Murrell studied the recombination of radical atoms in gas phase by using, as a model, a spherical box containing eight atoms [3], in which a uniform spherical shell, containing the centers of Lennard–Jones particles, was placed at the boundary. The adiabatic wall produces a radial force, which acts on the particles in the box. Few years later, Tenenbaum *et al*. [15] developed a method for studying the dynamics of particles in thermal gradients using a hard stochastic wall, which allows a particle to cross the simulation boundary and re–enter the box by reflection off the wall with a random thermal velocity. In this approach, the interactions of the particles in the simulation box with those outside were not included. Karplus and coworkers [5] argued that the method could produce spurious effects due to the simplistic boundary.

At about the same time, Berkowitz and McCammon [4] developed a SBP with stochastic boundaries in which the simulation box was decomposed into a *static* region of fixed particles and a *dynamic* region in which particles are allowed to move. The dynamic region was further divided into a core zone where the particles move according to Newtonian dynamics, and a buffer zone (thermal sink/source) where the particles move according to Langevin dynamics. The particles in the core zone interact with those in the static region and the entire system moves with the particle positioned at the centre of the system. Berkowitz and McCammon's method was further developed by Brooks and Karplus [5] by introducing a *soft* stochastic boundary and the *mean field force approximation* (MFFA). In MFFA, the interaction force between the particles in the core region and those outside it is obtained by integrating over all contributions to the average force due to the particles located outside the simulation box. However, the MFFA does not take into account the long–range electrostatic interactions due to the polar character of some compounds. These long–range interactions were included in the surface–constrained all–atom solvent (SCAAS) method proposed by King and Warshel [6] and in the reaction field with exclusion (RFE) method of Rullmann and van Duijnen [7].

More recently, Beglov and Roux [9] introduced a new SBP by separating the multidimensional solvent–solute partition function into an inner part, that describes the solute and a few layers of

solvent molecules, and an outer part. These authors showed that the SBP obtained by this separation is in fact the solvation energy of the supramolecular ensemble composed of the solute and the surrounding cluster of solvent molecules. This model differs from previous SBP models in that the cavity of the solute–solvent cluster can fluctuate to accommodate changes in solvent density and volume during dynamic simulation. In addition, the cavity wall is transparent to the inner molecules, but prevents outer molecules from getting inside. The long–range electrostatic interactions due to solvent polarization are treated using the reaction field method [16]. Im *et al*. [10] further developed this SBP into a *generalized* solvent boundary potential (GSBP) which is more appropriate for the investigation of the reaction regions in large enzymes. In another relatively recent development Essex and Jorgensen [8] proposed an empirical boundary potential similar to the dynamic surface boundary conditions method (DSBC) proposed by Juffer and Berendsen [17].

Darden *et al*. [18] analyzed the effect of replacing the PBC (with Ewald summation) with spherical boundary conditions (SBC, with the Born equation) on the solvation free energy of ions in water. For SBC they employed the SBP developed by Essex and Jorgensen [8] and introduced a correction scheme to evaluate accurately the solvation free energy of a cluster of molecules by using the Born equation. Their radial work function (essentially a reaction field potential) seems to play the same role as the discontinuity in the electric field across the dielectric interface obtained from the Poisson equation. Their method is useful for MD programs (*e.g*. AMBER), which use the Born equation (instead of the Poisson–Boltzmann equation) to correct the long–range electrostatics when cutoffs are used in simulations.

2 THE DEVELOPMENT OF THE SOLVENT BOUNDARY POTENTIAL

This paper describes the theoretical framework of a SBP that can be used in molecular dynamic simulations of systems composed of large enzymes with a small number of solvent molecules localized around a reaction site or a region of interest (*e.g*. in folding studies). The new SBP combines the stochastic buffer approach of Berkowitz and McCammon [4], with the MFFA of Brooks and Karplus [5], and the reaction field method with some additional ideas (*e.g*. Green's function decomposition method) from the work of Im *et al*. [10]. The details of this new SBP are presented in the next section. The implementation of this methodology into GROMACS molecular dynamics simulation package is still a work in progress.

2.1 The Deformable Boundary and the MFFA

Following earlier ideas from Stace and Murrell [3] and Berkowitz and McCammon [4], Brooks and Karplus [5] divided the system into *simulation* and *boundary* regions. The simulation region was further subdivided into *reaction* and *stochastic* buffer zones. They introduced a *deformable* boundary force (the mean field force, MFF) by further assuming that part of the force acting on

particles within the inner zone (reaction + buffer) arises from the average structure of the solvent in the outer (boundary) region. Hence, this force, $F_B(\mathbf{r}_0)$ on a particle located at position $\mathbf{r}_0$, is obtained by integrating the potential energy (U) gradient weighted by the probability $\rho g(\mathbf{r})$ of finding the other particles at position $\mathbf{r}$ in the outer region:

$$F_B(\mathbf{r}_0) = \int_{V-v} d\mathbf{r} \frac{\partial U}{\partial \mathbf{r}} \rho g(\mathbf{r}) \tag{1}$$

The integral in Eq. (1) is performed on the outer region volume (V–v). The boundary force acting on a particle decreases to zero as that particle in the inner region approaches the centre of the inner zone. The term "deformable boundary" means that solvent molecules in the inner region are allowed to cross the boundary to some extent, rather than being repelled by a hard–wall boundary as in Stace and Murrell's [3] method.

Brooks and Karplus [5] incorporated thermal and density fluctuations for the simulation zone [4] by defining a buffer region where the molecules move according to Langevin dynamics. Thus, the additional force on a particle, F_+, located at position $\mathbf{r}_0$ (r_0 = the distance from the centre of inner region) depends on whether the particle is located in the inner region, ($r_0 < R_B$, R_B = the radius of the buffer), the stochastic buffer region ($R_B < r_0 < R$, R = the radius of the deformable boundary) or beyond the boundary ($r_0 > R$) in the outer region:

$$F_+ = \begin{cases} F_B(\mathbf{r}_0), & r_0 \le R \\ F_B(\mathbf{r}_0) - \beta v(t) + f(t), & R_B < r_0 \le R \\ F_B^L(\mathbf{r}_0) - \beta v(t) + f(t), & R_B < r_0 \le R \end{cases} \tag{2}$$

where $-\beta v(t)$ is a dissipative force (β = friction coefficient) and $f(t)$ a random force. The random force is a Gaussian white noise source with the properties:

$$\begin{cases} \langle \mathbf{f}(t) \rangle = 0 \\ \langle \mathbf{f}(t) \cdot \mathbf{f}(0) \rangle = 6 k_B T \beta \delta(t) \end{cases} \tag{3}$$

which obeys the fluctuation–dissipation theorem. k_B is the Boltzmann constant, T the absolute temperature, and $\delta(t)$ the delta function.

When particles enter the outer region, the force on them is modified in such a way that is repulsive (F_B^L). This ensures that the particles are softly pushed back into the inner region and the average density of the solvent in the inner region remains constant during the simulation. To accomplish this the force due to the solvent continuum is modified ($F_B^L(\mathbf{r}_0)$) according to the approach suggested by Brooks and Karplus [5]. An alternative strategy will be the following: instead of modifying the boundary force (as in Eq. 2), a 'virtual' molecule (ion) is created randomly in the boundary region and pushed with random velocity in random direction into the buffer region. This virtual particle becomes real, and the molecule (ion) that crosses into the boundary region is 'annihilated'. The exchange free energy due to boundary crossing can be evaluated exactly as the

difference in the 'solvation' free energy of the exchanged particles in the 'buffer medium' (*i.e.* sum of cavity formation + particle–particle interaction). The dynamics obtained with these two strategies will be compared during the validation of the new SBP. A side effect of the latter strategy is that ion exchange through boundary enhances the effect of dielectric saturation and electrostriction [19–22], but should make the dynamics more realistic. If successful, the new strategy for handling particle exchange through the boundary will become an important methodological contribution to the development of the new SBP.

2.2 The Separation of the Configurational Partition Function

Beglov and Roux [9] proposed a new method for performing molecular dynamics simulations without PBC, in which the SBP is effectively identified with the solvation free energy (G_{sol}) of an effective super–cluster composed of the solute and those solvent molecules treated explicitly, *i.e.* located in the inner region:

$$G_{sol} = G_{cav} + G_{vdw} + G_{elec} \tag{4}$$

where G_{cav} is the work required to create an empty inner region, with G_{vdw} and G_{elec} being the free energies resulting from charging the inner region molecules with van der Waals and electrostatic interactions [23].

The starting point in obtaining the SBP is the splitting of the multiconfigurational partition function, Z, into parts corresponding to inner and outer regions through a clever renumbering scheme:

$$Z = \int d(\mathbf{X}_u) \frac{1}{n!} \int d(1)...d(\mathbf{n}) \times \frac{1}{(N-n)!} \int_{V-v} d(\mathbf{n}+1)...d(\mathbf{N}) e^{-U/k_B T} \tag{5}$$

where the vector $\mathbf{X}_{\mathrm{u}}$ contains the solute degrees of freedom, 1...**n** are the degrees of freedom of solvent molecules in the inner region, **n** + 1...**N** are the degrees of freedom of solvent molecules in the outer region, V and v are the volumes of the entire system and the inner region, respectively, U is the potential energy of the system.

While the theoretical approach is sound, its implementation is not without difficulties as noted by Beglov and Roux. Thus, in a simulation of a cluster of water molecules, Beglov and Roux [9] found an 'orientational bias' of the water molecules in the vicinity of the hard–wall that wraps the inner region (the boundary). While the hard–wall is 'transparent' for the molecules in the inner region, its presence is still 'felt' by these molecules and this spurious effect is a drawback of Beglov and Roux's SBP, which is difficult to overcome (*vide infra*). The orientational effect may stem from the fact that when a molecule gets more distant from the centre of the inner region empty shells are added to the cavity and this increases the cavity formation free energy (a positive energy term in Eq. 4), which leads to 'artificial' desolvation. To correct for this artifact the authors introduced an angular potential, that only partially removes the orientational bias [9].

The definition of the SBP introduced by Beglov and Roux is straightforward and appealing from a theoretical point of view, but the origin of its artifacts are not yet well understood. On the other hand, the MFFA with the deformable stochastic boundary method of Brooks and Karplus [5] provides an alternative description of the SBP, because it was successful in emulating full MD simulations. For this reason, the deformable stochastic boundary method was selected as the starting point for the development of the new SBP presented in this paper. This method will be combined with the method of Im *et al*. [10] for treating the electrostatic interactions (calculation and storage) between the inner and outer region molecules. Some modifications of previous approaches will also be described.

2.3 Green's Function Decomposition Algorithm for Electrostatic Interactions

David and Field [24] were the first to suggest the idea of using a set of basis functions to represent the electrostatic potential of a charge distribution ρ, together with an integral equation approach for solving the Poisson equation for the electrostatic potential. They also used Gaussian basis functions to spread atomic point charges on a finite region of space. Thus, instead of solving the differential equation (the Poisson equation) in the electrostatic potential, these authors used a *variational* approach by minimizing a free energy functional in the electrostatic potential. Their work bears some similarities with the newly proposed method of Im *et al*. [10] for the definition of a generalized solvent boundary potential (GSBP) for use in molecular dynamics simulations of very large protein/solvent systems. But the two methodologies share only the idea of using basis functions for describing point charges and a Green's function approach for solving the Poisson equation. Otherwise they are quite different both in scope and formal details. A brief description of the Im *et al*. method will be given here because this approach seems suitable for an efficient implementation of a non–PBC MD simulation algorithm.

Following previous developments introduced by Berkowitz and McCammon [4], Roux and coworkers [9,10] also split the simulation system (biopolymer + solvent molecules) into *inner* and *outer* regions. The inner region contains part of the biopolymer and those solvent molecules involved in the dynamics, while the outer region contains the rest of biopolymer atoms and solvent molecules, the latter in the form of a polarizable continuum. The key aspect of this method is the splitting of the total electrostatic interaction in the system into *static* and *dynamic* components. The static component includes contributions from the interaction between the point charges of biopolymer atoms located in the outer region and the reaction field potential induced by these charges into the polarizable continuum solvent. This component of the electrostatic interaction does *not* depend on the dynamics in the inner region and thus is evaluated only once (at the beginning of the simulation) and added as a constant term to the total electrostatic interaction energy. This procedure should drastically reduce the simulation time for large proteins because the majority of the protein atoms lay in the outer region. The dynamic component has two parts: the interaction

between atomic point charges located inside the inner region and the inter–regional interaction between inner– and outer–region atomic point charges. Both interactions depend on the instantaneous positions of the solvent molecules and inner region biopolymer atoms during simulation. The electrostatic interaction energy between outer and inner atomic point charges, E^{io}, is evaluated using the electrostatic potential generated by the atomic point charges in the outer region (*i.e.* those from protein atoms in the outside region):

$$E^{io} = \sum_{\alpha \in inner} q_\alpha \phi^o(\mathbf{r}_\alpha) \tag{6}$$

where q_α are the atomic point charges at $\mathbf{r}_\alpha$, and ϕ^o is the electrostatic potential generated by the solvent–screened atomic point charges located in the outer region. One of the novelties of this method is that ϕ^o is calculated only once and stored on a three dimensional grid constructed in the inner region for efficient evaluation of the electrostatic interaction energy during simulation.

A second novelty of this method is the separation of a static component of the interaction between inner–region atomic point charges, by using a Green's function decomposition technique [10]. This can be done by representing the set of point charges inside the inner region as a charge density $\rho(\mathbf{r})$ using a set of normalized basis functions $b_m(\mathbf{r})$:

$$\rho(\mathbf{r}) = \sum_m c_m b_m(\mathbf{r}) \tag{7}$$

where the coefficients c_m of the basis functions b_m are given by:

$$c_m = \sum_n S^{-1}_{nm} Q_n \tag{8}$$

with S_{nm} being the elements of the overlap matrix and Q_n the generalized multipole moments:

$$\begin{aligned} S_{nm} &= \int d\mathbf{r} b_n(\mathbf{r}) b_m(\mathbf{r}) \\ Q_n &= \sum_{\alpha \in inner} q_\alpha b_n(\mathbf{r}_\alpha) \end{aligned} \tag{9}$$

The electrostatic interaction energy E^{ii} due to the mutual interaction of inner–region charges (written in terms of generalized electrical multipoles) is:

$$\begin{aligned} E^{ii} &= \sum_{mn} Q_m \left[\sum_{ij} S^{-1}_{im} M_{ij} S^{-1}_{jn} \right] Q_n \\ M_{ij} &= \int d\mathbf{r} d\mathbf{r}' b_i(\mathbf{r}) G(\mathbf{r},\mathbf{r}') b_j(\mathbf{r}') \end{aligned} \tag{10}$$

where $G(\mathbf{r},\mathbf{r}')$ is the Green's function. The elements of matrix **M** are calculated only once and then are stored and used to evaluate E^{ii} during the simulation. This method, while effective in calculating the electrostatic interaction, requires a spherical or rectangular inner box with a smooth dielectric interface because in this way either spherical harmonics or Cartesian Legendre polynomials (which are orthogonal) can be used as basis functions for the charge distributions and thus avoid the

inversion of the overlap matrix in Eq. (8), a step which can be very expensive as the number of basis functions increases with the size of the inner region and the need for an accurate representation of the charge distribution in this region. The details of the calculation of the matrix elements of **M** are given in Roux and coworkers's paper about the development of GSBP [10].

Here one proposes a modification of the above algorithm that saves memory by eliminating the three dimensional grid (used to solve and store the electrostatic potential due to the outer charges), and increases the accuracy of calculating the electrostatic interaction between the inner– and outer–region charges. The increase in accuracy is a result of obtaining a smooth function for the electrostatic potential instead of using the discrete one with values on a grid, which also eliminates the requirement of spreading the inner region charges on the three dimensional grid (as required by the finite difference method [25]). In fact, the new approach uses the idea introduced by David and Field [24] for solving the Poisson equation by means of an integral equation approach. Thus, the basis functions $b_n(\mathbf{r})$ (introduced in Eq. (7)) representing charges in the inner region, are also used to expand the electrostatic potential created by the outer region point charges, as follows:

$$\phi^o(\mathbf{r}) = \sum_n d_n b_n(\mathbf{r}) \tag{11}$$

David and Field showed that the electrostatic potential, $\phi(\mathrm{r})$, that satisfies the Poisson equation:

$$\nabla \cdot \left[\varepsilon(\mathbf{r}) \nabla \phi(\mathbf{r})\right] = -4\pi\rho(\mathbf{r}) \tag{12}$$

minimizes the following free energy functional:

$$G = \int d\mathbf{r} \left[\rho(\mathbf{r})\phi(\mathbf{r}) - \frac{\varepsilon(\mathbf{r})}{8\pi} \left(\nabla \phi(\mathbf{r})\right)^2 \right] \tag{13}$$

where $\varepsilon(\mathrm{r})$ is the dielectric function. Eq. (13) defines the variational principle that can be used to determine the variational coefficients d_n in Eq. (11) such that the electrostatic potential ϕ^o is the solution of the Poisson Eq. (12). The resultant matrix equation obtained by substituting Eq. (11) into Eq. (13) is:

$$\begin{aligned} G &= \sum_i d_i P_i - \sum_i \sum_j d_i d_j F_{ij} \\ P_i &= \int d\mathbf{r} \rho(\mathbf{r}) b_i(\mathbf{r}) \\ F_{ij} &= \int d\mathbf{r} \frac{\varepsilon(\mathbf{r})}{8\pi} \left[\nabla b_i(\mathbf{r})\right] \cdot \left[\nabla b_j(\mathbf{r})\right] \end{aligned} \tag{14}$$

In this particular case the Poisson equation (Eq. 12) reduces to the Laplace equation because the charges in the inner region are not considered for the calculation of ϕ^o, that is to say, the **P** vector (Eq. 14) is zero. The value of the dielectric function $\varepsilon(\mathbf{r})$ is equal to one in the inner region. The coefficients d_n must be constrained such that the electrostatic potential follows the Laplace equation:

$$\sum_i d_i K_i = \sum_i \frac{d_i}{4\pi} \int d\mathbf{r} \nabla \cdot \left[\varepsilon(\mathbf{r}) \nabla b_i(\mathbf{r}) \right] = 0 \tag{15}$$

The minimization of Eq. (14) under the constraints given in Eq. (15) leads to the following solution for the expansion coefficients:

$$\mathbf{d} = -\frac{\lambda}{2} \mathbf{F}^{-1} \mathbf{K} \tag{16}$$

where λ is a Lagrange multiplier. The coefficients d_n are determined once and used all over the simulation. The required storage is of the order of the number of basis functions instead of n^3 (n is the number of grid points in one dimension). An alternative of this method is to calculate the electrostatic potential on the grid as suggested by Roux and coworkers and subsequently fit the grid value potentials to the basis functions. This requires the use of the three dimensional grid only at the beginning of the simulation, and the memory can be reused later by re–allocation. The fitted electrostatic potential may not be as accurate as the one obtained by the variational method. Both variants require the inversion of a matrix and they should be equally computationally efficient, but the fitting procedure still requires the electrostatic potential to be obtained from the Poisson equation. This makes the first variant, that uses the integral equation approach, a better choice.

2.4 Inclusion of Polarizable Dipoles for Atoms Located in the Outer Region of the Biopolymer

The next step in improving the description of the electrostatic interaction between the solvent–screened atomic charges in the inner– and outer–regions is to add polarizable point dipoles on atoms both in the inner– (if treated by molecular mechanics) and the outer–region. This will take into account the polarization effects of the moving solvent molecules and protein atoms in the inner–region, on the protein atoms in the outer–region. A method that implements polarizable dipoles in hybrid quantum mechanical–molecular mechanical (QM/MM) force fields was described by Bakowies and Thiel [26]. Their implementation will be used for the SBP proposed here.

2.5 Treatment of Dielectric Saturation and Electrostriction Effects

Dielectric saturation (the orientation of water dipoles around ions/polar molecules) and electrostriction (increased water density around ions/polar molecules) largely compensate each other energetically [20], but the electrostriction leads to a net change in volume when the ionic concentration varies. This effect should be relatively small for the Brooks–Karplus strategy for handling particle exchange across the boundary, because ions that cross the boundary are quickly pushed back. Electrostriction may be important for the new strategy proposed here because in this case the fluctuation of ionic concentration may have a larger periodicity. One way to avoid the density fluctuation due to electrostriction is to shrink/expand the buffer region when ions cross the boundary.

The change in volume due to electrostriction (excess volume) can be calculated using the radial distribution function (Eq. (20) in Ref. [20]) obtained from the compressibility model of ionic solvation [20]. The position of the boundary after ion crossing is determined by calculating a new radius for the spherical cavity (which defines the cavity of the inner + buffer region, Figure 1) in such a way that the shell volume obtained by reducing/extending the cavity radius equals the change in volume due to ion exchange (excess volume, V_{ex} in Figure 1). This procedure will only require the calculation of the surface area of that part of the cavity, which interfaces with the solvent continuum (Figure 1).

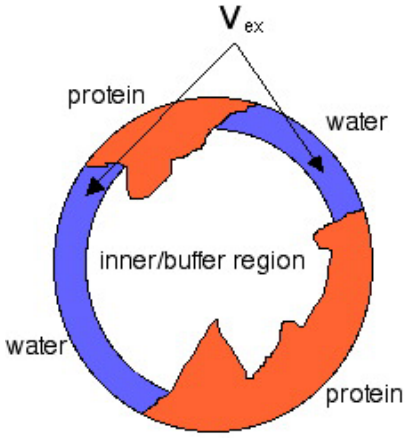

Figure 1. The change in the inner/buffer region volume (V_{ex}) due to interface crossing by ions.

It was shown by many researchers [19–22], that dielectric saturation and electrostriction effects for ions solvated in a dielectric continuum are reasonably taken into account by the linear response theory when the ionic radii are adjusted accordingly (Born theory). Incorporation of these effects into the new SBP, may not be necessary, because in our methodology ions are annihilated (or pushed back) when cross into continuum, and their contribution to the ionic strength of the continuum is handled by the Debye–Hückel theory [27] as implemented in the Poisson–Boltzmann equation method [25]. But, when the cavity is charged (due to charged amino acids and other ions), then the dielectric saturation and electrostriction effects must be taken into account because the radius which will compensate for these effects is not known. To account for the electrostriction effect of the charged inner–buffer region on system energy, the pressure–dependent compressibility model of ionic solvation, $HI_{кр}$ developed by Ichiye and coworkers [20] will be implemented into the new SBP.

3 TESTING THE SOLVENT BOUNDARY POTENTIAL

The new SBP will be implemented in GROMACS and its performance will be compared with the SBP developed by Roux and coworkers [9,10]. A series of tests are proposed here for the evaluation of the performance of the new SBP.

3.1 The Solvation of One Water Molecule

MD simulations (using Newton's equation of motion) of about 1 ns will be performed on spheres containing 25, 50 then 100 water molecules. The SBP simulation results (*i.e*. the pair correlation function for O–O and O–H intermolecular distances, the velocity autocorrelation function, self–diffusion coefficient, normalized local density and temperature profiles) will be compared with full MD of a box of 216 water molecules and with the results for the Langevin dynamics for solvating one water molecule from the work of Beglov and Roux [9]. As noted by these authors, their implementation of the SBP introduces an orientational bias of the water molecules near the boundary (the hard wall, see Figure 4 in Ref. [9]). Beglov and Roux suggested that this artifact results from the approximations made in the van der Waals (ΔW_{vdw}) and electrostatic components (ΔW_{elec}) of the potential of the mean force (PMF) derived for the SBP. The orientational bias was not noticed by Brooks and Karplus in their simulations using the SBP with a stochastic deformable boundary [5]. The hard wall in Beglov and Roux's SBP is not transparent and is actually acting on the molecules located in the inner region which probably produces this orientational bias. The approximations in ΔW_{vdw} and ΔW_{elec} components of the PMF introduced by these authors may not be responsible for this artifact, after all. It is very probable that the introduction of the stochastic deformable boundary proposed by Brooks and Karplus [5] will remove the orienational bias. The tests on the solvation of one water molecule will show how well the new SBP reproduces the thermal and structural characteristics of the bulk water as compared with full simulations and if the new SBP is successful in removing the orientational bias of the molecules near the solvent boundary noticed by Beglov and Roux [9].

3.2 Solvation of Ions

In the second test, the structure of the solvent molecules around the solvated ions such as, Na^+, K^+ or Ca^{2+} will be determined with the new SBP method for spheres of 25, 50 and 100 water molecules, and the ion–water oxygen pair correlation function will be compared with the full MD simulations and the results obtained by Beglov and Roux. (see Figure 7 in Ref. [9]) The solvation free energy will be calculated using standard free energy perturbation techniques [28,29]. We will follow the same protocol as Beglov and Roux for calculating the cavity formation energy (scaling Lennard–Jones parameter σ) and interaction energy (scaling the Lennard–Jones parameter ε and the partial atomic charges). The results will be compared with the experimental solvation free energies for these ions. The Lennard–Jonnes parameters for Na^+ and K^+ as given by Beglov and Roux (see Table 1 in Ref. [9]) will be used as a first guess but will eventually be adjusted to reproduce experimental solvation free energies.

3.3 The PMF for *n*–Butane

In a third test, the potential of the mean force (PMF) for different values of the C–C–C–C dihedral angle in *n*–butane will be calculated using the new SBP method, the full MD simulation

results will be compared with those obtained by Beglov and Roux [9]. The aim of this test is to see if the new SBP correctly indicates that the *cis* conformer is 0.45 kcal/mol more stable than the *trans* conformer in solution. The PMF will be calculated for systems containing 25 and 100 water molecules. Beglov and Roux results suggest that the conformational barrier is reproduced well even with only 25 water molecules (see Figure 8 in Ref. [9]).

3.4 MD Simulation of Angiotensin II

The octapeptide angiotensin II (AngII: NRVYVHPF), is a key hormone in the regulation of blood pressure and in salt and water homeostatis [30]. Its role is regulated by AT_1 and AT_2 receptors (members of the G–protein–coupled superfamily) [31]. This peptide and an analogue (NRCYCHPF has a disulfide–bridge) [32] were chosen to test whether the inclusion of polarizable dipoles for atoms in the inner + buffer region will affect the dynamics (change in conformation) of this peptide in water. The bioactive conformation of AngII is U–shaped [31,32].

3.5 MD Simulation of Myoglobin

Oxymyoglobin (PDB: 1A6M) was selected to test whether the inclusion of polarizable dipoles for protein atoms located in the boundary changes significantly the dynamics of the O_2–bound heme and His64 (known to assist in O_2 binding) [33] This test is particularly useful for further investigating NOS, which is a heme protein, too. Spherical inner+buffer regions of 15, 20, and 30 Å will be created around Fe. Polarizable dipoles will be placed on protein atoms located in a 5 Å shell around the buffer region. 1 ns MD simulations will be carried out for each region size. The distance between O_2 and His64 will be monitored during the trajectory and the results will be compared with the full MD simulation

3.6 MD Simulation of Nitric Oxide Synthase

The ultimate goal of the development of this new SBP is to use it to perform simulations of enzymes that have hundred of thousands of atoms. One of these applications will be to perform simulations on the nitric oxide synthase (NOS) in water and to use simulation snapshots in the investigation of NO synthesis reaction mechanism.

The biochemical reactivity of nitric oxide (NO) is very complex and has many implications in cell life, which makes NO one of the most experimentally studied molecules in biomedical sciences [34]. NO released from stimulated endothelial cells causes vascular–muscle relaxation and inhibits platelet aggregation via activation of guanylate cyclase. NO is also produced in response to inflammatory processes and can inhibit DNA synthesis and the metabolism of cancer cells by interfering with essential iron–sulfur–containing mitochondrial enzymes [35]. NO can also have damaging effects [36]. For example, excessive NO synthesis induced in blood vessels leads to vascular leakage and dramatic drop in blood pressure. Inappropriate inflammatory response leads to tissue damage, and in stroke NO may contribute to brain damage (Alzheimer and Parkinson

diseases [37]). Thus, the understanding of the chemistry of NO, the mechanism of NO synthesis and the reaction of NO with different molecular targets in living cell, is an essential step toward controlling its activity. NOS enzymes are heme (iron–porphyrin) proteins that resemble P_{450} protein [38]. NOS uses 3 electrons acquired from the reductase domain (NADPH – the reduced form of nicotinamide adenine dinucleotide phosphate) and oxidize arginine to citrulline and NO in two reaction steps: (1) arginine to N–hydroxyarginine (NHA) and (2) NHA to citrulline [39]. These enzymes are expressed in endothelium cells, macrophages in neurons, among others. There are three isotypes of NOS enzymes, nNOS, eNOS and iNOS [40]. All of them seem to use the same mechanism for the synthesis of NO.

The X–ray crystal structure of the complex of arginine, N–hydroxyarginine, and citrulline with the oxygenase domain of eNOS (endothelium NOS) obtained at 1.9 Å by Raman *et. al*. [41] (the protein data bank ID–1NSE) will be used as starting structures for the simulation. MD simulations of 1 ns will be performed with the new SBP method on three complexes of the enzyme oxygenase domain with arginine, N–hydroxyarginine, and citrulline. Snapshots (at 5 ps intervals) from the trajectory will be taken. These snapshots will be further classified into clusters with similar geometries. The similarity between two configurations is measured by the root mean square difference between the internal coordinates of those configurations. Energetically weighted statistical average representations will be selected for each cluster. These representatives will be used later as starting points for exploring the potential energy surface (PES) through QM/MM calculations. The crystal structures for the oxygenase part of NOS enzyme (from endothelium eNOS) with and without the H_4B cofactor published by Raman *et al*. (at 1.9 Å resolution [41]) will be used. The oxygenase part (in dimer form) is divided into an inner part that contains the active site and a 10 Å layer of residues plus the backbone that surrounds the active site (that includes the heme cofactor), the substrate (arginine), the oxygen molecule, surrounding water molecules and the H_4B cofactor. The outer–region contains the rest of the protein atoms that are used only in the first stage to calculate the electric field that acts on the inner region. The outer–region also contains the continuum solvent.

A modification of GROMACS program is necessary in order to include the long–range electrostatics using a dielectric continuum description of the solvent and the contribution from the outer–protein atoms. First, hydrogen atoms are added to the crystal structure of the protein, and a constrained–minimization is performed to relax the protein and remove the imperfections in the crystal structure, or bad contacts introduced by adding the hydrogen atoms. Next the protein is divided into inner– and outer–regions. The inner–region is centered on the heme group. A new minimization is performed to relax the newly inserted water molecules, and after that the system will be equilibrated for around 100 ps (the time for equilibration will be investigated). The time necessary for a simulation will be investigated. MD snapshots will be clustered and analyzed, and representative configurations will be selected for the QM/MM calculations.

According to the two–step mechanism for arginine oxidation [42] twelve starting structures will be defined and used for MD simulation. These input structures are: **1** Free enzyme (without tetrahydrobiopterin cofactor, H_4B), **2** Enzyme with H_4B bound, **3** Enzyme (Fe^{3+}) with arginine and H_4B bound, **4** Enzyme (Fe^{2+}) with O_2, arginine and H_4B bound, **5** Enzyme (Fe^{3+}–O–O^-) with arginine and H_4B bound, **6** Enzyme $(FeO)^{3+}$ with arginine and H_4B bound, **7** Enzyme (Fe^{3+}) with NHA and H_4B bound, **8** Enzyme (Fe^{3+}–O–O^-) with NHA and H_4B bound, **9** Enzyme–intermediate 1, **10** Enzyme–intermediate 2, **11** Enzyme–intermediate 3, **12** Enzyme (Fe^{3+}) with citrulline, NO and H_4B bound.

4 CONCLUSIONS

This paper proposes a new solvent boundary potential for use in the computer simulations of very large systems. The new SBP distinguishes from previous methodologies by combining the MFFA with the Green's function approach for treating short– and long–range interactions. In addition, the new SBP introduces a new strategy for dealing with electrostriction effects due to ion crossing of the solvent boundary, and proposes a new technique based on the integral equation approach for solving for the electrostatic potential due to atoms positioned outside the simulation box, and due to solvent continuum. One of the strength of the SBP is the fact that it does *not* produce spurious artifacts (as PBC) and thus can be applied to inhomogeneous systems as membranes and composite materials. While the implementation of a SBP is more laborious than the PBC, the calculations with SBP should be much faster because of the drastic reduction in the number of particles taken into account in calculation. The use of SBP in the computer simulation of very large systems (of hundred of thousands of atoms) is probably the only method of choice nowadays, thus new and more efficient algorithms are required to make the SBP a computational efficient methodology. Work in this direction is in progress in our group.

Acknowledgment

The author acknowledges the financial support (startup fund) of this work by the Cleveland State University.

5 REFERENCES

[1] M. P. Allen and D. J. Tildesley, *Computer Simulation of Liquids*, Oxford Science Publications: Clanderon, Oxford, 1989.
[2] A. R. Leach, *Molecular Modeling. Principles and Applications*, 1st ed.; Addison Wesley Longman: London, 1996.
[3] A. J. Stace and J. N. Murrel, Molecular Dynamics and Chemical Reactivity: A Computer Study of Iodine Atom Recombination under High Pressure Conditions, *Mol. Phys*. **1977**, *33*, 1–24.
[4] M. Berkowitz and J. A. McCammon, Molecular Dynamics with Stochastic Boundary Conditions, *Chem. Phys. Lett*. **1982**, *90*, 215–217.
[5] C. L. Brooks III and M. Karplus, Deformable Stochastic Bondary in Molecular Dynamics, *J. Chem. Phys*. **1983**, *79*, 6312–6325.
[6] G. King and A. Warshel, A Surface Constrained All–Atom Solvent Model for Effective Simulations of Polar

Solutions, *J. Chem. Phys*. **1989**, *91*, 3647–3661.
[7] J. A. Rullmann and P. T. van Duijnen, Analysis of Discrete and Continuum Dielectric Models; Application of the Calculation of Protonation Energies in Solution, *Mol. Phys*. **1987**, *61*, 293–311.
[8] J. W. Essex and W. L. Jorgensen, An Empirical Boundary Potential for Water Droplet Simulations, *J. Comp. Chem*. **1995**, *16*, 951–972.
[9] D. Beglov and B. Roux, Finite Representation of an Infinite Bulk System: Solvent Boundary Potential for Computer Simulations, *J. Chem. Phys*. **1994**, *100*, 9050–9063.
[10] W. Im, S. Berneche and B. Roux, Generalized Solvent Boundary Potential for Computer Simulation, *J. Chem. Phys*. **2001**, *114*, 2924–2937.
[11] D. A. Pearlman, D. A. Case, J. C. Caldwell, G. L. Seibel, U. C. Singh, P. Weiner and P. A. Kollman. Amber 4.1; 4.1 ed.; University of California: San Francisco, 1993.
[12] B. R. Brooks, R. E. Bruccoleri, B. D. Olafson, D. J. States, S. Swaminathan and M. Karplus, Charmm – a Program for Macromolecular Energy, Minimization, and Dynamics Calculations, *J. Comput. Chem*. **1983**, *4*, 187–217.
[13] W. F. van Gunsteren and H. J. C. Berendsen, Computer Simulation of Molecular Dynamics: Methodology, Applications, and Perspectives in Chemistry, *Angew. Chem. Int. Ed. Engl*. **1990**, *29*, 992–1023.
[14] S. H. Northrup, M. R. Pear, C. Y. Lee, J. A. McCammon and M. Karplus, Dynamical Theory of Activated Processes in Globular–Proteins, *Proc. Natl. Acad. Sci. USA* **1982**, *79*, 4035–4039.
[15] A. Tenenbaum, G. Ciccotti and R. Gallico, Stationary Non–Equilibrium States by Molecular–Dynamics – Fourier Law, *Phys. Rev. A* **1982**, *25*, 2778–2787.
[16] C. J. F. Bottcher, *Theory of Electric Polarization*, Elsevier Scientific Publishing Company: Amsterdam, 1973; Vol. 1.
[17] A. H. Juffer and H. J. C. Berendsen, Dynamic Surface Boundary–Conditions – a Simple Boundary Model for Molecular–Dynamics Simulations, *Mol. Phys*. **1993**, *79*, 623–644.
[18] T. Darden, D. Pearlman and L. G. Pedersen, Ionic Charging Free Energies: Spherical Versus Periodic Boundary Conditions, *J. Chem. Phys*. **1998**, *109*, 10921–10935.
[19] B. E. Conway, Electrolyte Solutions: Solvation and Structural Effects, *Annu. Rev. Phys. Chem*. **1966**, *17*, 481–528.
[20] J.–K. Hyun and T. Iciye, Nonlinear Response in Ionic Solvation: A Theoretical Investigation, *J. Chem. Phys*. **1998**, *109*, 1074–1083.
[21] I. Danielewicz–Ferchmin and A. R. Ferchmin, Hydration of Ions at Various Temperatures: The Role of Electrostrcition, *J. Chem. Phys*. **1998**, *109*, 2394–2402.
[22] C. S. Babu and C. Lim, Theory of Ionic Hydration: Insights from Molecular Dynamics Simulations and Experiment, *J. Phys. Chem. B* **1999**, *103*, 7958–7968.
[23] J. Tomasi and M. Persico, Molecular Interactions in Solution: An Overview of Methods Based on Continuous Distributions of the Solvent, *Chem. Rev*. **1994**, *94*, 2027–2094.
[24] L. David and M. J. Field, Basis Set Approach to Solution of Poisson Equation for Small Molecules Immersed in Solvent, *J. Comput. Chem*. **1997**, *18*, 343–350.
[25] A. Nicholls and B. Honig, A Rapid Finite Difference Algorithm, Utilizing Successive over–Relaxation to Solve the Poisson–Boltzmann Equation, *J. Comput. Chem*. **1991**, *12*, 435–445.
[26] D. Bakowies and W. Thiel, Hybrid Models for Combined Quantum Mechanical and Molecular Mechanical Approaches, *J. Phys. Chem*. **1996**, *100*, 10580–10594.
[27] D. A. McQuarrie, *Statistical Mechanics*, University Science Books: New York, 1976.
[28] T. P. Straatsma, H. J. C. Berendsen and J. P. M. Postma, Free–Energy of Hydrophobic Hydration – a Molecular–Dynamics Study of Noble–Gases in Water, *J. Chem. Phys*. **1986**, *85*, 6720–6727.
[29] T. P. Straatsma, H. J. C. Berendsen and J. P. M. Postma, Free–Energy of Ionic Hydration – Analysis of a Thermodynamic Integration Technique to Evaluate Free–Energy Differences by Molecular–Dynamics Simulations, *J. Chem. Phys*. **1988**, *89*, 5876–5886.
[30] F. M. Bumpus and M. C. Khosla, Angiotensin Analogs as Determinants of the Physiological Role of Angiotensin and Its Metabolite, In *Hypertension: Physiology and Treatment*; Genest, J., Koiw, E., Kuchel, O., Eds.; McGraw–Hill: New York, 1977; pp 183–201.
[31] S. S. Karnik, A. Husain and R. M. Graham, Molecular Determinants of Peptide and Non–Peptide Binding of the AT1 Receptor, *Clinic. Exper. Pharm. Phys*. **1996**, *Suppl 3*, S58–S66.
[32] G. V. Nikiforovich and G. R. Marshall, 3d Model for Tm Region of the at–1 Receptor in Complex with Angiotensin II Independently Validated by Site–Directed Mutagenesis Data, *Biochem. Biophys. Res. Comm*. **2001**, *286*, 1204–1211.
[33] C. K. Mathews and K. E. van Holde, *Biochemistry*, The Benjamin/Cummings Publishing Company: Menlo Park, 1996.
[34] J. MacMicking, Q. Xie and C. Nathan, Nitric Oxide and Macrophage Function, *Annu. Rev. Immunol*. **1997**, *15*, 323–350.

[35] G. C. Brown, Nitric Oxide and Mitochondrial Respiration, *Biochim*. *Biophys*. *Acta* **1999**, *1411*, 351–369.
[36] M. P. Murphy, Nitric Oxide and Cell Death, *Biochim*. *Biophys*. *Acta* **1999**, *1411*, 401–414.
[37] J. P. Bolanos and A. Almedia, Roles of Nitric Oxide in Brain Hypoxia–Ischemia, *Biochim*. *Biophys*. *Acta* **1999**, *1411*, 415–436.
[38] K. A. White and M. A. Marletta, Nitric Oxide Synthase Is a Cytochrome P–450 Type Hemoprotein, *Biochemistry* **1992**, *31*, 6627–6631.
[39] J. F. Kerwin Jr., J. R. Lancaster Jr. and P. L. Feldman, Nitric–Oxide – a New Paradigm for 2nd–Messengers, *J*. *Med*. *Chem*. **1996**, *38*, 4344–4362.
[40] D. Stuehr, Mammalian Nitric Oxide Synthases, *Biochim*. *Biophys*. *Acta* **1999**, *1411*, 217–230.
[41] C. S. Raman, H. Li, P. Martasek, V. Kral and B. S. S. Masters, Crystal Structure of Constitutive Endothelial Nitric Oxide Synthase: A Paradigm for Pterin Function Involving a Novel Metal Center, *Cell* **1998**, *95*, 939–950.
[42] M. A. Marletta, Nitric–Oxide Synthase Structure and Mechanism, *J*. *Biol*. *Chem*. **1993**, *268*, 12231–12234.

Biographies

Valentin Gogonea is assistant professor of chemistry at Cleveland State University, OH. He obtained his MS in 1982 in organic chemistry at Polytechnic Institute of Timisoara, Romania, and his Ph.D. in 1996 in computational chemistry from Toyohashi University of Technology, Toyohashi, Japan in the group of professor Eiji Osawa. Between 1996–1997 he was an Alexander von Humboldt fellow and worked with professor Paul von Ragué Schleyer at Erlangen–Nürnberg University, Erlangen, Germany and from 1998–2001 he was a postdoctoral associate with professor Kenneth M. Merz, Jr. at The Pennsylvania State University.